niques developed in relation to RDFT can be used with the other transforms and vice versa. All the transforms can also be computed with basically the same hardware.

Recently, we have generalized the results presented in this paper to DCT. It turns out that DCT is a weighted sum of $G_1(\cdot)$ and $G_0(\cdot)$ after proper permutations of input data. Further generalizations to other trigonometric transforms [11] are in progress. These results will be published in subsequent papers.

REFERENCES

[1] A. K. Jain, "A fast Karhunen-Loeve transform for finite discrete images," in *Proc. Nat. Electron. Conf.*, Chicago, IL, Oct. 1974, pp. 323-328.

[2] N. Ahmed, T. Natarajan, and K. R. Rao, "Discrete cosine transform," *IEEE Trans. Comput.*, pp. 90-93, Jan. 1974.

[3] O. Ersoy, "A real formalism of discrete Fourier transform in terms of skew-circular correlations and its computation by fast correlation techniques," presented at the SPIE Conf. 431, Real Time Signal Processing VI, San Diego, CA, Aug. 1983.

[4] H. Kitajima, "A symmetric cosine transform," *IEEE Trans. Comput.*, vol. C-29, pp. 317-323, Apr. 1980.

[5] W. Chen, C. H. Smith, and S. C. Fralick, "A fast computational algorithm for the discrete cosine transform," *IEEE Trans. Commun.*, vol. COM-25, pp. 1004-1009, Sept. 1977.

[6] M. J. Narasimha and A. M. Peterson, "On the computation of the discrete cosine transform," *IEEE Trans. Commun.*, vol. COM-26, pp. 934-936, June 1978.

[7] P. Yip and K. R. Rao, "On the computation and the effectiveness of discrete sine transform," *Comput. Elec. Eng.*, vol. 7, pp. 45-55, 1980.

[8] —, "A fast computational algorithm for the discrete sine transform," *IEEE Trans. Commun.*, vol. COM-28, pp. 304-307, Feb. 1980.

[9] H. T. Kung, "Special purpose devices for signal and image processing: An oppurtunity in very large scale integration (VLSI)," *SPIE*, vol. 241, Real Time Signal Processing III, 1980.

[10] H. J. Nussbaumer, *Fast Fourier Transform and Convolution Algorithms*. New York: Springer-Verlag, 1982.

[11] A. K. Jain, "A sinusoidal family of unitary transforms," *IEEE Trans. Pattern Anal. Machine Intell.*, vol. PAMI-1, pp. 356-365, Oct. 1979.

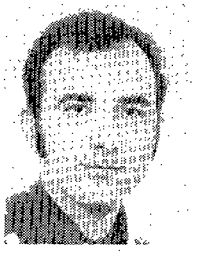

Okan Ersoy was born in Istanbul, Turkey, on September 5, 1945. He received the B.S.E.E. degree from Robert College in 1967, and the M.S., Certificate of Engineering, second M.S., and Ph.D. degrees from the University of California, Los Angeles, in 1968, 1971, and 1972, respectively.

He was a Teaching and Research Assistant in the Department of Electrical Sciences and Engineering Department, UCLA (1967-1972), Assistant Professor in the Department of Electrical Engineering, Bosphorus University (1972-1973), and Associate Professor in the second semesters at the same university (1976-1980). He joined the Central Institute for Industrial Research, Oslo, Norway, as a Researcher in the Applied Mathematics and Systems Science Division in 1973. He was a Visiting Scholar at UCSD from 1980-1981. His current interests include digital and optical signal and image processing, parallel processing of information, pattern recognition, transform and convolution techniques, VLSI systems in these areas, and applied mathematics.

Dr. Ersoy is a member of the Optical Society of America, the Norwegian Society for Scientists and Engineers, and the New York Academy of Sciences.

Convergence Analysis of LMS Filters with Uncorrelated Gaussian Data

ARIE FEUER AND EHUD WEINSTEIN

***Abstract*—Statistical analysis of the least mean-squares (LMS) adaptive algorithm with uncorrelated Gaussian data is presented. Exact analytical expressions for the steady-state mean-square error (mse) and the performance degradation due to weight vector misadjustment are derived. Necessary and sufficient conditions for the convergence of the algorithm to the optimal (Wiener) solution within a finite variance are derived. It is found that the adaptive coefficient μ, which controls the rate of convergence of the algorithm, must be restricted to an interval significantly smaller than the domain commonly stated in the literature. The outcome of this paper, therefore, places fundamental limitations on the mse performance and rate of convergence of the LMS adaptive scheme.**

Manuscript received October 1, 1983; revised February 29, 1984.

A. Feuer is with the Department of Electrical Engineering, Technion, Haifa, Israel.

E. Weinstein is with the Department of Oceanic Engineering, Woods Hole Oceanographic Institute, Woods Hole, MA 02543, and also with the Department of Electronic Systems, Faculty of Engineering, Tel Aviv University, Israel.

I. INTRODUCTION

EARLY studies on the convergence of the least mean-square (LMS) algorithm concentrated on the necessary conditions required for the weight vector mean to converge to the optimal (Wiener) solution (e.g., [1], [2]). These conditions do not however, guarantee, a finite variance for the weight vector, neither do they guarantee finite mean-square error (mse). Hence, as many users of the algorithm realized, considerably more stringent conditions were required to ensure convergence of the algorithm.

The need to study the convergence properties of the weight vector convariance matrix was identified by Horowitz and Senne [3]. They derived a recursive equation characterizing the transient response of the covariance matrix and found

0096-3518/85/0200-0222$01.00

necessary and sufficient conditions for the convergence of this equation. Unfortunately, these results are not the focus of [3], hence overlocked by many readers.

Our purpose in this paper is twofold. We intend to highlight the results in [3] by deriving them in a different way. Then, carry the study further by translating the convergence conditions into bounds on the adaptation coefficient μ. In addition, an exact analytical expression for the steady-state mse and a new measure for the rate of convergence of the algorithm are derived.

A parallel set of results is also obtained for the partially adaptive LMS algorithm introduced by Griffiths [4]. The two algorithms are then compared on the basis of their convergence properties and their steady-state mse performance.

II. Steepest Descent (SD), Least Mean-Square (LMS), and the Modified Least Mean-Square (MLMS) Algorithms

The basic system of interest here is illustrated in Fig. 1, where $\boldsymbol{X}(k)$ is the data vector at the kth time instant, $\boldsymbol{W}$ is a vector of constant weights, $d(k)$ the desired (training) signal, and $y(k)$ represents its estimate. The problem is to find $\boldsymbol{W}$ which minimizes the mse, namely,

$$\epsilon = E\{e^2(k)\} = E\{(d(k) - y(k))^2$$
$$= E\{(d(k) - \boldsymbol{W}^T\boldsymbol{X}(k))^2\}$$

where $E\{\ \}$ stands for the statistical expectation of the bracketed quantity. If $\boldsymbol{X}(k)$ and $d(k)$ are jointly stationary, then

$$\epsilon = E\{d^2(k)\} - 2\boldsymbol{W}^T\boldsymbol{r} + \boldsymbol{W}^T R\,\boldsymbol{W} \tag{1}$$

where

$$\boldsymbol{r} = E\{\boldsymbol{X}(k)\,d(k)\} \tag{2}$$

and

$$R = E\{\boldsymbol{X}(k)\,\boldsymbol{X}(k)^T\}. \tag{3}$$

Since ϵ is a quadratic functional of $\boldsymbol{W}$, it has a unique minimum (whenever R is nonsingular) obtained by choosing

$$\boldsymbol{W}^* = R^{-1}\boldsymbol{r}. \tag{4}$$

This is the well-known Wiener solution. Substituting (4) into (1), the minimum attainable mse is given by

$$\epsilon^* = E\{d^2(k)\} - \boldsymbol{r}^T R^{-1}\boldsymbol{r}. \tag{5}$$

To avoid a direct inversion of R, an iterative solution can be used, based upon a gradient-following method. The resulting algorithm, known as the steepest descent (SD) algorithm, is characterized by the equation

$$\boldsymbol{W}(k+1) = (I - 2\mu R)\,\boldsymbol{W}(k) + 2\mu\boldsymbol{r} \tag{6}$$

where $\boldsymbol{W}(k)$ is the weight vector of the kth iteration cycle and μ is a constant gain which controls the rate of convergence of the algorithm. It has been shown [1], [2] that $\boldsymbol{W}(k)$ converges to $\boldsymbol{W}^*$ as $k \to \infty$ so long as

$$0 < \mu < \frac{1}{\lambda_{\max}} \tag{7}$$

where $\lambda_{\max}$ denotes the largest eigenvalue of R.

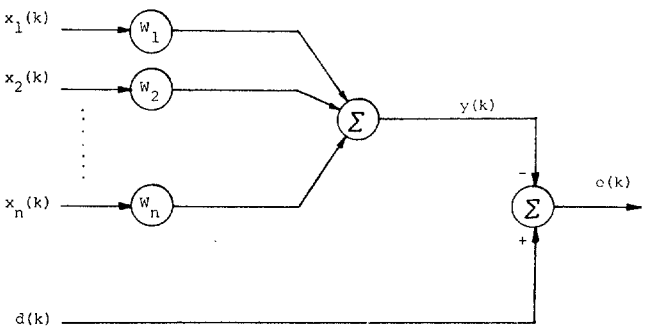

Fig. 1.

In many practically interesting situations, prior knowledge of $\boldsymbol{r}$ and R is not available. In that case the matrix quantities appearing in (2) and (3) can be replaced by their instantaneous estimates $\boldsymbol{X}(k)\,d(k)$ and $\boldsymbol{X}(k)\,\boldsymbol{X}(k)^T$, respectively. This is a common procedure in stochastic approximation. The resulting equation is given by

$$\boldsymbol{W}(k+1) = (I - 2\mu\boldsymbol{X}(k)\,\boldsymbol{X}(k)^T)\,\boldsymbol{W}(k) + 2\mu d(k)\,\boldsymbol{X}(k)$$
$$= \boldsymbol{W}(k) + 2\mu e(k)\,\boldsymbol{X}(k) \tag{8}$$

This is Widrow's well-known LMS algorithm [1], [2].

In [4] Griffiths addresses the problem where no reference signal is available but the cross-correlation vector $\boldsymbol{r}$ is known. The algorithm presented in [4] is obtained by simply substituting $\boldsymbol{X}(k)\,\boldsymbol{X}(k)^T$ for R in (6). One obtains

$$\tilde{\boldsymbol{W}}(k+1) = (I - \boldsymbol{X}(k)\,\boldsymbol{X}^T(k))\,\tilde{\boldsymbol{W}}(k) + 2\mu\boldsymbol{r}. \tag{9}$$

The Griffiths algorithm can be viewed as a cross between the SD and LMS and will be referred to as the modified LMS (MLMS) algorithm.

In both the LMS and MLMS, $\boldsymbol{W}(k)$ is obtained through a stochastic equation. It is, in general, a random vector quantity. Its relation to the optimal (Wiener) solution can therefore be measured only in a statistical sense.

If we assume that the various $\boldsymbol{X}(k)$, $k = 0, 1, 2, \cdots$ are statistically independent, then $\boldsymbol{W}(k)$ is independent of $\boldsymbol{X}(k)$ and the weight vector mean for both the LMS and MLMS satisfies (6). One, therefore, concludes that both algorithms are asymptotically unbiased (i.e., $E\{\boldsymbol{W}(k)\} \to \boldsymbol{W}^*$ as $k \to \infty$) as long as the adaptation coefficient μ satisfies (7).

However, as was recognized in [3] and pointed out in the introduction section, considerably more stringent conditions than those given by (7) are required to ensure the convergence of the weight vector covariance matrix, hence, the resulting mse. This is the subject of the next section.

III. Convergence of the LMS and the MLMS

Before we proceed, let us introduce some notation which will be used throughout the remainder of the paper. Since R is symmetric there exists a unitary transformation U (where $U^T = U^{-1}$) such that

$$URU^T = \Lambda = \text{diag}\,[\lambda_1, \lambda_2, \cdots \lambda_n] \tag{10}$$

λ_i are the eigenvalues of R. Let

$$\boldsymbol{V}(k) = U(\boldsymbol{W}(k) - \boldsymbol{W}^*) \tag{11}$$

$$\boldsymbol{M}(k) = E\{\boldsymbol{V}(k)\} \tag{12}$$

and

$$C(k) = E\{\boldsymbol{V}(k)\,\boldsymbol{V}^T(k)\}. \tag{13}$$

The above notation will be used for the LMS scheme. Similar notation with "~" will be used for the MLMS.

Using the assumption that the various data vectors are mutually independent, together with an additional assumption that $\boldsymbol{X}(k)$ is zero mean and Gaussian, Horowitz and Senne [3] derived the following recursive equation satisfied by $C(k)$:

$$C(k+1) = C(k) - 2\mu[\Lambda C(k) + C(k)\Lambda] + 8\mu^2\Lambda C(k)\Lambda + 4\mu^2 \operatorname{tr}[\Lambda C(k)]\,\Lambda + 4\mu^2\epsilon^*\Lambda \tag{14}$$

where tr [ ] stands for the trace of the bracketed matrix. The matrix equation (14) can be decomposed into the following n^2 scalar equations:

$$C_{ii}(k+1) = \rho_{ii}C_{ii}(k) + 4\mu^2\lambda_i \sum_{p=1}^{n} \lambda_p C_{pp}(k) + 4\mu^2\epsilon^*\lambda_i \tag{15}$$

and for $i \neq j$

$$C_{ij}(k+1) = \rho_{ij}C_{ij}(k) \tag{16}$$

where $C_{ij}(k)$ is the (i,j) element of $C(k)$ and

$$\rho_{ij} = 1 - 2\mu(\lambda_i + \lambda_j) + 8\mu^2\lambda_i\lambda_j. \tag{17}$$

Since $C_{ij}^2(k) \leq C_{ii}(k)\,C_{jj}(k)$, the convergence of the diagonal elements of $C(k)$ ensures the convergence of the off-diagonal elements. We shall, therefore, concentrate on (15). Concatenating the n equation into a vector form, one obtains

$$\boldsymbol{\sigma}(k+1) = F\boldsymbol{\sigma}(k) + 4\mu^2\epsilon^*\boldsymbol{\lambda} \tag{18}$$

where

$$\boldsymbol{\sigma}(k) = [C_{11}(k), C_{22}(k), \cdots, C_{nn}(k)]^T \tag{19}$$

$$F = \operatorname{diag}[\rho_1, \rho_2, \cdots, \rho_n] + 4\mu^2\boldsymbol{\lambda}\boldsymbol{\lambda}^T \tag{20}$$

and

$$\boldsymbol{\lambda} = [\lambda_1, \lambda_2, \cdots, \lambda_n]^T. \tag{21}$$

Following similar considerations for the MLMS scheme one finds (see Appendix)

$$\tilde{\boldsymbol{\sigma}}(k+1) = F\tilde{\boldsymbol{\sigma}}(k) + 4\mu^2 g(k) \tag{22}$$

where $\tilde{\boldsymbol{\sigma}}(k)$ consists of the diagonal elements of $\tilde{C}(k)$ and $g(k)$ is defined in (A7). It can easily be observed that $g(k)$ is bounded whenever μ satisfies (7). Hence, the convergence of both $\boldsymbol{\sigma}(k)$ and $\tilde{\boldsymbol{\sigma}}(k)$ depends on the matrix F. Both will converge if and only if the eigenvalues of F are all within the unit circle. The eigenvalues of F are the solution of the following equation in α

$$\det[F - \alpha I]\ 0 \tag{23}$$

where det [ ] is the determinant of the bracketed matrix. Now

$$\begin{aligned}
\det[F - \alpha I] &= \det\{\operatorname{diag}(\rho_1 - \alpha, \rho_2 - \alpha, \cdots, \rho_n - \alpha) + 4\mu^2\boldsymbol{\lambda}\boldsymbol{\lambda}^T\} \\
&= \det\{\operatorname{diag}(\rho_1 - \alpha, \rho_2 - \alpha, \cdots, \rho_n - \alpha)\} \cdot \det\left[I + 4\mu^2 \operatorname{diag} \cdot \left[\frac{1}{\rho_1 - \alpha}, \frac{1}{\rho_2 - \alpha}, \cdots, \frac{1}{\rho_n - \alpha}\right]\boldsymbol{\lambda}\boldsymbol{\lambda}^T\right] \\
&= \left[\sum_{j=1}^{n}(\rho_j - \alpha)\right]\left[1 + 4\mu^2\boldsymbol{\lambda}^T \operatorname{diag} \cdot \left[\frac{1}{\rho_1 - \alpha}, \cdots, \frac{1}{\rho_n - \alpha}\right]\boldsymbol{\lambda}\right] \\
&= \left[\prod_{j=1}^{n}(\rho_j - \alpha)\right]\left[1 + 4\mu^2\sum_{j=1}^{n}\frac{\lambda_j^2}{\rho_j - \alpha}\right]
\end{aligned} \tag{24}$$

where for notational convenience we define $\rho_j \triangleq \rho_{jj}$. Since the common denominator of the sum of terms $\sum_{j=1}^{n}\lambda_j^2/(\rho_j - \alpha)$ is $\prod_{j=1}^{n}(\rho_j - \alpha)$, one needs only to consider the equation

$$f(\alpha) = 1 + 4\mu^2\sum_{j=1}^{n}\frac{\lambda_j^2}{\rho_j - \alpha} = 0. \tag{25}$$

Clearly, the poles of $f(\alpha)$ are the ρ_j's and from (17)

$$\rho_j = 1 - 4\mu\lambda_j + 8\mu^2\lambda_j^2 = (1 - 2\mu\lambda_j)^2 + 4\mu^2\lambda_j^2 > 0. \tag{26}$$

Hence, the various poles of $f(\alpha)$ are placed on the positive real axis. We further observe that

$$\frac{df(\alpha)}{d\alpha} = 4\mu^2\sum_{j=1}^{n}\frac{\lambda_j^2}{(\rho_j - \alpha)^2} > 0 \tag{27}$$

$f(\alpha)$ must therefore assume the general form illustrated in Fig. 2. Between each pair of successive poles, $f(\alpha)$ has a single zero. If we arrange the poles in an increasing order, i.e., $0 < \rho_1 < \rho_2 < \cdots < \rho_n$, then[1]

$$0 < \rho_1 < \alpha_1 < \rho_2 < \alpha_2 < \cdots < \alpha_{n-1} < \rho_n < \alpha_n \tag{28}$$

where α_j's are the zeros of $f(\alpha)$, hence the eigenvalues of F. The last inequality in (28) can easily be explained by observing that $f(\alpha)$ never crosses zero to the left of ρ_1, thus the nth zero-crossing must occur to the right of ρ_n. Hence, if we require that $\alpha_n < 1$, all the eigenvalues of F will be located within the unit circle. From Fig. 2 one immediately observes that $\alpha_n < 1$ if and only if

$$\rho_j < 1, \quad j = 1, 2, \cdots, n$$

and

$$f(\alpha)\big|_{\alpha=1} = 1 + 4\mu^2\sum_{j=1}^{n}\frac{\lambda_j^2}{\rho_j - 1} > 0. \tag{29}$$

Substitution of (17) into (29) yields the following necessary

[1]For every λ_s which has multiplicity $M_s > 1$, F has $M_s - 1$ eigenvalues equal to ρ_s.

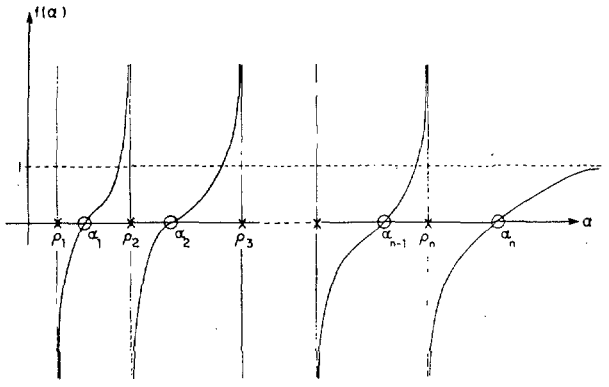

Fig. 2.

and sufficient conditions

$$0 < \mu < \frac{1}{2\lambda_j}, \quad j = 1, 2, \cdots, n \tag{30a}$$

and

$$\sum_{j=1}^{n} \frac{\mu\lambda_j}{1 - 2\mu\lambda_j} < 1. \tag{30b}$$

These are the same conditions as given in [3].

It is of important practical interest to translate conditions (30) into direct bounds on the adaptive coefficient μ. To do this we first observe that the left-hand side of (30b) is a strictly monotonically increasing function of μ which has singularities at $1/2\lambda_j$, $j = 1, 2, \cdots, n$ and is equal to zero for $\mu = 0$. Hence, if we let μ_j denote the solutions of the equation

$$\sum_{j=1}^{n} \frac{\mu\lambda_j}{1 - 2\mu\lambda_j} = 1, \tag{31}$$

we have, very much like in (28), assuming the λ_j's are ordered $\lambda_1 \leqslant \lambda_2 \leqslant \cdots \leqslant \lambda_n$,

$$0 < \mu_1 < \frac{1}{2\lambda_n} < \mu_2 < \frac{1}{2\lambda_{n-1}} < \cdots < \mu_n < \frac{1}{2\lambda_1}.$$

Then, it is clear that the condition

$$0 < \mu < \mu_1 = \min(\mu_j)$$

is equivalent to conditions (30).

In general, a closed form expression for μ_1 cannot be found. However, following the analytical considerations outlined in Appendix B, a tight lower bound on μ_1 is given by

$$\mu_1 \geqslant \frac{n}{\sqrt{3\sum_{j=1}^{n}\lambda_j + 9(n-1)^2\left[\sum_{j=1}^{n}\lambda_j\right]^2 - 8n(n-1)\sum_{i\neq j}^{n}\sum^{n}\lambda_i\lambda_j}} \triangleq \bar{\mu}. \tag{32}$$

A "safe" choice for μ is therefore any value in the interval

$$0 < \mu \leqslant \bar{\mu}. \tag{33}$$

For the case $n = 2$ (arbitrary λ_1 and λ_2) and the case $\lambda_j = \lambda$, $j = 1, 2, \cdots, n$, where μ_1 can be calculated analytically, it can easily be shown that $\bar{\mu}$ coincides with μ_1. In more complicated situations μ_1 cannot be calculated analytically, however, a set of numerical examples indicate that $\bar{\mu}$ is an extremely tight lower bound on μ_1. We note in passing, that condition (7) is very clearly dominated by (33).

We further observe that

$$\bar{\mu} \geqslant \frac{1}{3\sum_{j=1}^{n}\lambda_j} = \frac{1}{3\ \mathrm{tr}\ [R]}. \tag{34}$$

Hence a more conservative region is

$$0 < \mu \leqslant \frac{1}{3\ \mathrm{tr}\ [R]}. \tag{35}$$

The upper bound in (35) has a distinct practical advantage. tr $[R]$ is, by definition, the total average input signal power which can easily be estimated from the received signal.

IV. Steady-State Performances of the LMS

The overall efficiency of the LMS scheme can be measured by its steady-state mse and the rate of convergence of the algorithm. The mse at the kth iteration cycle, denoted by $\epsilon(k)$, is given by

$$\begin{aligned}\epsilon(k) &\triangleq E\{e^2(k)\} = E\{[d(k)^T - \boldsymbol{X}(k)^T\boldsymbol{W}(k)]^2\}\\ &= E\{[d(k) - \boldsymbol{X}(k)^T\boldsymbol{W}^* - \boldsymbol{X}(k)^T(\boldsymbol{W}(k) - \boldsymbol{W}^*)]^2\}\\ &= \epsilon^* - 2E\{\boldsymbol{X}(k)^T(\boldsymbol{W}(k) - \boldsymbol{W}^*)[d(k) - \boldsymbol{X}(k)^T\boldsymbol{W}^*]\}\\ &\quad + E\{(\boldsymbol{W}(k) - \boldsymbol{W}^*)^T\boldsymbol{X}(k)\boldsymbol{X}(k)^T(\boldsymbol{W}(k) - \boldsymbol{W}^*)\}.\end{aligned} \tag{36}$$

As the data vectors at distinct times are assumed to be uncorrelated as well as Gaussian, $\boldsymbol{X}(k)$ and $\boldsymbol{W}(k)$ are statistically independent. We further observe that $\boldsymbol{X}(k)$ and $[d(k) - \boldsymbol{X}(k)^T\boldsymbol{W}^*]$ are also mutually uncorrelated hence, independent. This is true since

$$E\{\boldsymbol{X}(k)[d(k) - \boldsymbol{X}(k)^T\boldsymbol{W}^*]\} = \boldsymbol{r} - R\boldsymbol{W}^* = 0. \tag{37}$$

Hence, in the second term of (36), $E\{\boldsymbol{X}(k)^T\}$ can be factored out. As $\boldsymbol{X}(k)$ is assumed to be zero mean, this term equals zero and we are left with

$$\begin{aligned}\epsilon(k) &= \epsilon^* + \mathrm{tr}\,[E\{\boldsymbol{W}(k) - \boldsymbol{W}^*)(\boldsymbol{W}(k) - \boldsymbol{W}^*)^T\}\\ &\quad \cdot E\{\boldsymbol{X}(k)\boldsymbol{X}(k)^T\}]\\ &= \epsilon^* + \mathrm{tr}\,[U^T C(k) UU^T \Lambda U]\\ &= \epsilon^* + \boldsymbol{\lambda}^T\boldsymbol{\sigma}(k).\end{aligned} \tag{38}$$

Assuming that μ is chosen so that $\boldsymbol{\sigma}(k)$ convergences to a finite value, one immediately obtains

$$\epsilon(\infty) = \epsilon^* + \boldsymbol{\lambda}^T\boldsymbol{\sigma}(\infty) \tag{39}$$

where from (18)

$$\boldsymbol{\sigma}(\infty) = 4\mu^2\epsilon^*(I - F)^{-1}\boldsymbol{\lambda}. \tag{40}$$

$\epsilon(\infty)$ is, by definition, the steady-state mse and ϵ^* is the minimum attainable mse (when $\boldsymbol{r}$ and R are known *a priori*). The second term in (39), therefore, represents the access mse due to weight vector misadjustment. A dimension-free measure for the degradation in performance is defined as (see [4], [5])

$$M_s = \frac{\epsilon(\infty) - \epsilon_*}{\epsilon_*}. \tag{41}$$

Substituting (39) and (40) into (41), one immediately obtains

$$M_s = 4\mu^2 \boldsymbol{\lambda}^T (I - F)^{-1} \boldsymbol{\lambda}. \tag{42}$$

The rate of convergence of the mse to its steady-state can be measured by the following sum

$$J = \sum_{k=0}^{\infty} [\epsilon(k) - \epsilon(\infty)] \tag{43}$$

with small J indicating fast convergence rate. Denoting

$$\boldsymbol{\Delta}(k) = \boldsymbol{\sigma}(k) - \boldsymbol{\sigma}(\infty) \tag{44}$$

we get from (39)

$$\epsilon(k) - \epsilon(\infty) = \boldsymbol{\lambda}^T [\boldsymbol{\sigma}(k) - \boldsymbol{\sigma}(\infty)] = \boldsymbol{\lambda}^T \boldsymbol{\Delta}(k). \tag{45}$$

Making use of (18) and (40) it can easily be shown that

$$\boldsymbol{\Delta}(k+1) = F\boldsymbol{\Delta}(k). \tag{46}$$

It follows that

$$J = \boldsymbol{\lambda}^T \sum_{k=0}^{\infty} \boldsymbol{\Delta}(k) = \boldsymbol{\lambda}^T \left(\sum_{k=0}^{\infty} F^k \right) \boldsymbol{\Delta}(o)$$
$$= \boldsymbol{\lambda}^T (I - F)^{-1} \boldsymbol{\Delta}(o). \tag{47}$$

Substituting (20) and (21) into (42) and (47) and some algebra[2] one finds

$$M_s = \frac{\sum_{i=1}^{n} \frac{\mu\lambda_i}{1 - 2\mu\lambda_i}}{1 - \sum_{i=1}^{n} \frac{\mu\lambda_i}{1 - 2\mu\lambda_i}} \tag{48}$$

$$J = \frac{1}{4} \frac{\sum_{i=1}^{n} \frac{[\Delta(o)]_i}{1 - 2\mu\lambda_i}}{\mu \left[1 - \sum_{i=1}^{n} \frac{\mu\lambda_i}{1 - 2\mu\lambda_i} \right]}. \tag{49}$$

One observes that M_s can be controlled through the choice of μ. The smaller μ is, the smaller M_s will be. On the other hand, a small μ may slow down the convergence of the algorithm as indicated by (49). There exists a value of μ resulting in the fastest convergence (smallest J) and up to this value there is a clear tradeoff in the choice of μ between steady-state mse and rate of convergence.

[2]To invert the matrix $(I - F)$ we have used the Bartlet formula given by

$$(\Gamma + \alpha \boldsymbol{u}\boldsymbol{u}^T)^{-1} = \Gamma^{-1} - \frac{\alpha}{1 + \alpha \boldsymbol{u}^T \Gamma^{-1} \boldsymbol{u}} \Gamma^{-1} \boldsymbol{u}\boldsymbol{u}^T \Gamma^{-1}$$

where Γ is a nonsingular matrix, $\boldsymbol{u}$ a vector, and α a scalar.

To find this optimal μ one may try to solve the equation

$$\frac{\partial J}{\partial \mu} = 0. \tag{50}$$

Note that the solution to (50) generally depends on the initial value $\boldsymbol{\Delta}(o)$, hence, of limited practical use. For the special case $\lambda_i = \lambda, i = 1, 2, \cdots, n$, (49) assumes the simplified form

$$J = \frac{1}{4} \frac{\sum_{i=1}^{n} [\Delta(o)]_i}{\mu [1 - \mu(n+2)\lambda]}. \tag{51}$$

Assuming that $\boldsymbol{\Delta}(o)$ is independent of μ, (51) is minimized by the choice

$$\mu^* = \frac{1}{2(n+2)\lambda}. \tag{52}$$

Equation (52) agrees with the result in [3], which was obtained from different considerations.

V. Comparison Between the LMS and MLMS

Following the same considerations for the MLMS one finds

$$\tilde{M}_s = \frac{\sum_{i=1}^{n} \frac{\mu g_i(\infty)}{(1 - 2\mu\lambda_i)\epsilon^*}}{1 - \sum_{i=1}^{n} \frac{\mu\lambda_i}{1 - 2\mu\lambda_i}} \tag{53}$$

where $g_i(k)$ is defined in Appendix A [see (A7)]. Since $\tilde{\boldsymbol{M}}(k) \to \boldsymbol{0}$ as $k \to \infty$, $g_i(\infty)$ is given by

$$g_i(\infty) = (r_i^o)^2 + \lambda_i \sum_{j=1}^{n} (r_j)^2 / \lambda_j \tag{54}$$

where r_i^o is the ith component of $\boldsymbol{r}^o = U\boldsymbol{r}$. Comparison between (48) and (53) reveals an interesting insight into the two algorithms. While M_s is completely independent of the amount of correlation between the data and the desired signal, $\tilde{M}_s$ is highly dependent on the components of $\boldsymbol{r}$. Thus, weak correlation (the information content of the data is small) will result in $\tilde{M}_s$ smaller than M_s, while with high correlation $\tilde{M}_s$ will exceed M_s. This phenomenon can be explained by looking at (8) and (9). By using $\boldsymbol{r}$ rather than its instantaneous estimate $\boldsymbol{X}(k)d(k)$, the MLMS is more "cautious" than the LMS. This pays off whenever $\boldsymbol{X}(k)d(k)$ is misleading in relation to $\boldsymbol{X}(k)\boldsymbol{X}(k)^T$, in other words, whenever the correlation between $\boldsymbol{X}(k)$ and $d(k)$ is weak. The conclusion from the above discussion is that if one does have the choice and both $d(k)$ and $\boldsymbol{r}$ are available, LMS should be preferred when the correlation is high and MLMS when it is low.

VI. Simulation Results

To demonstrate and support our analysis, extensive simulations were carried out on the computer. The case we are considering here is likely to occur in passive sonar applications.

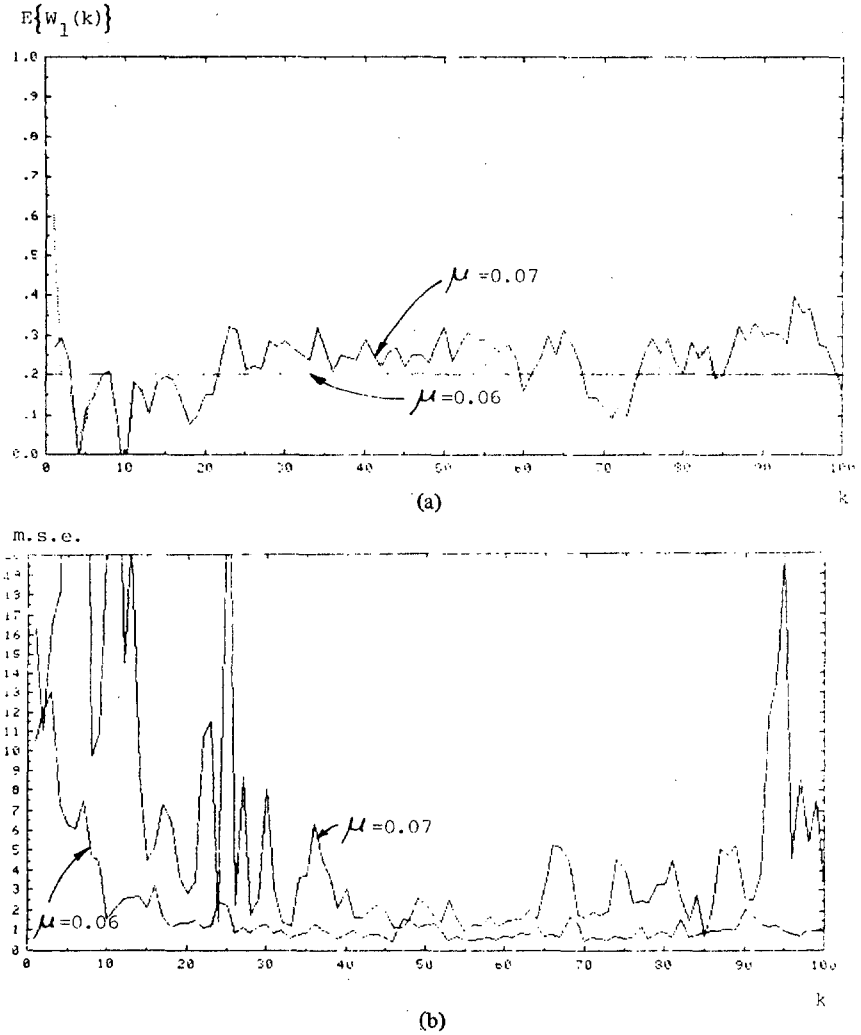

Fig. 3.

Let the data vector be presented by

$$X(k) = \begin{bmatrix} x_1(k) \\ x_2(k) \\ x_3(k) \\ x_4(k) \end{bmatrix} = \begin{bmatrix} s(k) + n_1(k) \\ s(k) + n_2(k) \\ s(k) + n_3(k) \\ s(k) + n_4(k) \end{bmatrix} \tag{55}$$

and the reference (training) signal be given by

$$d(k) = \alpha s(k) + (1 - \alpha^2)^{1/2}\, n(k). \tag{56}$$

$s(\cdot)$, $n_i(\cdot)$, $n(\cdot)$ are sample functions from mutually uncorrelated zero-mean white Gaussian sequences. The $n_i(k)$'s have unit variance; $s(k)$ and $n(k)$ have a variance of σ^2. $o \leqslant \alpha \leqslant 1$ will be used to control the correlation between $X(k)$ and $d(k)$ while preserving the power of $d(k)$.

Fig. 3 presents averages of ten independent runs using the LMS algorithm on random data generated by the computer for the case $\sigma = 1$ and $\alpha = 1$. From Fig. 3(a) it is clear that for both $\mu = 0.06$ and $\mu = 0.07$ the weight vector mean converges (only the first component is presented, but it is typical to the others). The conclusion concerning Fig. 3(b) is very different; while for $\mu = 0.06$ the resulting mse converges, for $\mu = 0.07$ it does not. These observations are consistent with our analysis.

The eigenvalues of R are $\lambda_1 = \lambda_2 = \lambda_3 = 1$, $\lambda_4 = \lambda_{max} = 1 + 4\sigma^2$. To ensure convergences of the weight vector mean, one requires only that $\mu < 1/\lambda_{max} = 0.2$. However, the convergence of the weight vector covariance, hence, the resulting mse, is guaranteed only when

$$\mu < \bar{\mu} = \frac{1}{3(1 + \sigma^2 + \sqrt{9\sigma^4 + 2\sigma^2 + 1})} \tag{57}$$

and for $\sigma = 1$, $\bar{\mu} = 0.0610$. We note in passing that the exact bound of μ can also be calculated here from (31) and is found to be $\mu_1 = 0.0613$.

In Fig. 4 the tradeoff between rate of convergence and steady-state performance is illustrated. The curves in this figure were generated recursively using (18) and (38).

The existence of an optimal μ (from a convergence rate point of view) is demonstrated in Fig. 5. The curve in this figure corresponds to a choice of initial conditions such that $[\Delta(o)]_i = \Delta$, $i = 1, 2, \cdots, n$. Hence, $\mu^* \approx 0.035$ is an optimal choice only in that neighborhood; however, the basic trend is clear.

In Fig. 6 we compare the mse performance of the LMS and MLMS using the recursive equations developed in the analysis. With a high degree of correlation between $X(k)$ and $d(k)$ ($\alpha = 1$), the LMS clearly outperforms the MLMS [Fig. 6(a)],

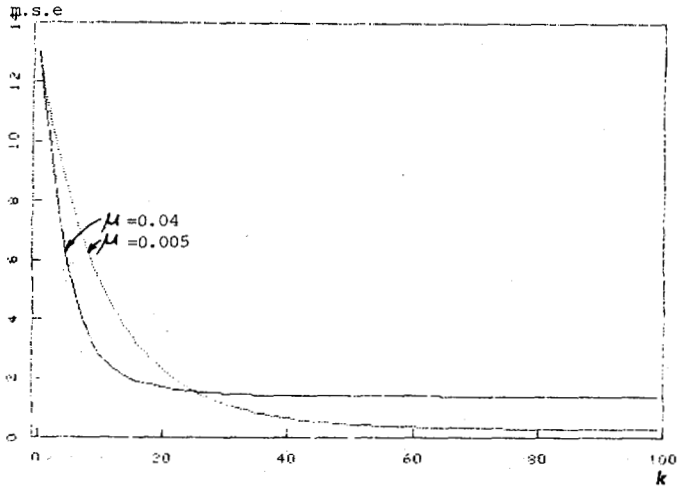

Fig. 4.

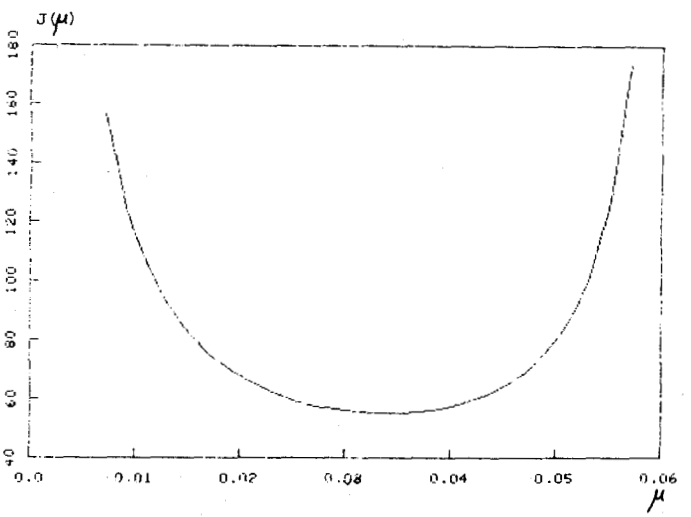

Fig. 5.

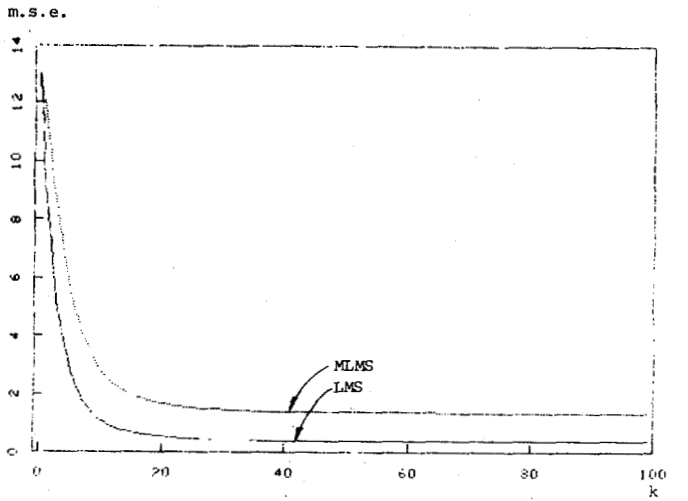

(a) $\alpha = 1.0$

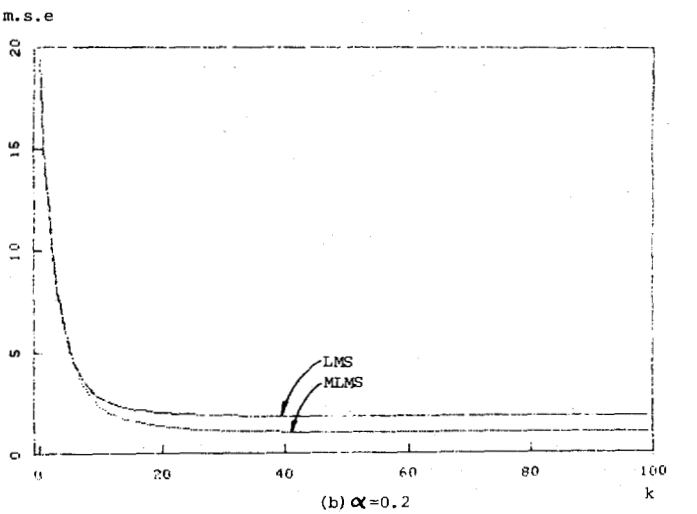

(b) $\alpha = 0.2$

Fig. 6.

while with a low degree of correlation ($\alpha = 0.2$) the trend is reversed [Fig. 6(b)]. This is also demonstrated in Fig. 7, where the curves are obtained by averaging fifty independent simulation results on computer generated random data.

VII. Conclusions

Convergence analysis of the LMS adaptive algorithm with uncorrelated Gaussian data is presented. Necessary and sufficient conditions under which the weight vector converges to the optimal (Wiener) solution within a finite variance are established. These conditions are then translated into bounds on the adaptation coefficient μ. These bounds are found to be significantly smaller than those required for the weight vector mean to converge. Exact analytical expressions for the steady-state mse and the performance degradation due to weight vector misadjustment are derived.

A new measure for the rate of convergence of the algorithm (for comparison purposes mainly) is suggested. This measure is then used to demonstrate the tradeoff between steady-state mse and convergence rate. The existence of an optimal μ which maximizes the rate of convergence is also demonstrated.

The LMS scheme is compared with a more "conservative" algorithm proposed by Griffiths [4]. The LMS turns out to be superior when the correlation between the received data and the desired (training) signal is high and inferior when the degree of correlation is low.

Appendix A

Using the notation defined by (10) through (13), (9) can be rewritten in the form

$$\tilde{\boldsymbol{V}}(k+1) = (I - 2\mu \boldsymbol{X}^o(k)\boldsymbol{X}^{oT}(k))\,\tilde{\boldsymbol{V}}(k) + 2\mu e_o(k) \qquad \text{(A1)}$$

where

$$\boldsymbol{X}^o(k) = U\boldsymbol{X}(k),\ \boldsymbol{r}^o = U\boldsymbol{r},\ \boldsymbol{W}^o = U\boldsymbol{W}^* = \Lambda^{-1}\boldsymbol{r}^o \qquad \text{(A2)}$$

and

$$e_o(k) = \boldsymbol{r}^o - \boldsymbol{X}^o(k)\boldsymbol{X}^{oT}(k)\boldsymbol{W}^o. \qquad \text{(A3)}$$

Note that

$$E\{e_o(k)\} = \boldsymbol{r}^o - \Lambda\Lambda^{-1}\boldsymbol{r}^o = 0. \qquad \text{(A4)}$$

Following the same considerations leading to (14) (see [3]

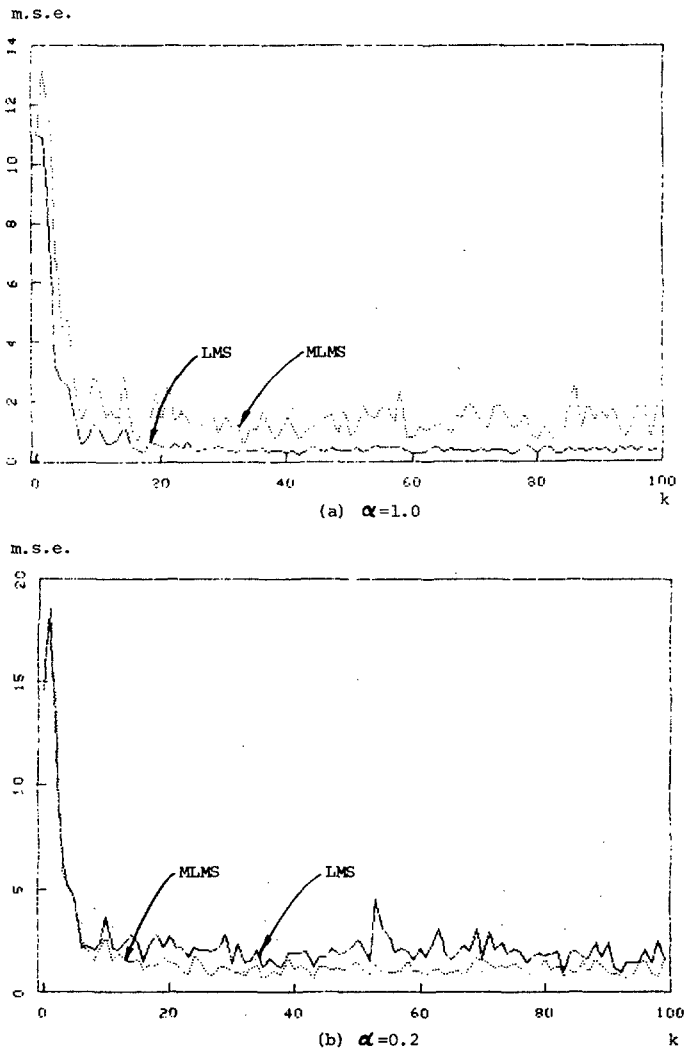

Fig. 7.

for details), one finds

$$\begin{aligned}\tilde{C}(k+1) &= \tilde{C}(k) - 2\mu[\Lambda\tilde{C}(k) + \tilde{C}(k)\Lambda] \\ &\quad + 4\mu^2\{2\Lambda\tilde{C}(k)\Lambda + \mathrm{tr}[\Lambda\tilde{C}(k)]\Lambda\} \\ &\quad + 4\mu^2\{\boldsymbol{r}^o\boldsymbol{r}^{oT} + r^{oT}\Lambda^{-1}\boldsymbol{r}^o\Lambda + \boldsymbol{r}^o\tilde{\boldsymbol{M}}(k)^T\Lambda \\ &\quad + \Lambda\tilde{\boldsymbol{M}}(k)\boldsymbol{r}^{oT} + 2\tilde{\boldsymbol{M}}^T(k)\boldsymbol{r}^o\Lambda\}. \end{aligned} \tag{A5}$$

From (A5), one immediately obtains

$$\tilde{\boldsymbol{\sigma}}(k+1) = F\tilde{\boldsymbol{\sigma}}(k) + 4\mu^2\boldsymbol{g}(k) \tag{A6}$$

where $\tilde{\boldsymbol{\sigma}}(k)$ consists of the diagonal components of $\tilde{C}(k)$ and $\boldsymbol{g}(k)$ is the vector whose ith component is given by

$$\begin{aligned} g_i(k) &= (r_i^o)^2 + \lambda_i \sum_{j=1}^{n} (r_j^o)^2/\lambda_j \\ &\quad + 2\lambda_i\left[r_i^o\tilde{M}_i(k) + \sum_{j=1}^{n} r_j^o\tilde{M}_j(k)\right]. \end{aligned} \tag{A7}$$

Appendix B

Let $\mu_1 \leqslant \mu_2 \leqslant \cdots \leqslant \mu_n$ be the solution to (31). Our objective is to set a lower bound on μ_1. To do that let us rewrite (31) in the form

$$\begin{aligned}&\left(\frac{1}{\mu}\right)^n - a_1\left(\frac{1}{\mu}\right)^{n-1} + a_2\left(\frac{1}{\mu}\right)^{n-2} - \cdots + (-1)^n a_n \\ &\quad = \prod_{j=1}^{n}\left(\frac{1}{\mu} - \frac{1}{\mu_j}\right) = 0 \end{aligned} \tag{B1}$$

where by direct comparison with (31) one observes that

$$a_1 = 3\sum_{j=1}^{n}\lambda_j, \qquad a_2 = 4\sum_{i\neq j}^{nn}\lambda_i\lambda_j. \tag{B2}$$

In this setting $1/\mu_1$ is the largest root of (B1). A theorem developed in [5] asserts that $1/\mu_1$ can be closely bounded from above by

$$\frac{1}{\mu_1} \leqslant \frac{1}{\mu} = \frac{1}{n}\left[s_1 + \sqrt{(n-1)(ns_2 - s_1^2)}\right] \tag{B3}$$

where

$$s_1 = \sum_{j=1}^{n}\frac{1}{\mu_j} \tag{B4}$$

and

$$s_2 = \sum_{j=1}^{n}\left(\frac{1}{\mu_j}\right)^2 = \left[\sum_{j=1}^{n}\frac{1}{\mu_j}\right]^2 - \sum_{i\neq j}^{nn}\frac{1}{\mu_i}\cdot\frac{1}{\mu_j}. \tag{B5}$$

By comparing the first and second versions of (B1), one immediately obtains

$$\sum_{j=1}^{n}\frac{1}{\mu_j} = a_1, \qquad \sum_{i\neq j}^{nn}\frac{1}{\mu_i}\cdot\frac{1}{\mu_i} = a_2. \tag{B6}$$

It follows that

$$s_1 = a_1 = 3\sum_{j=1}^{n}\lambda_j \tag{B7}$$

$$\begin{aligned} s_2 &= a_1^2 - 2a_2 \\ &= 9\left[\sum_{j=1}^{n}\lambda_j\right]^2 - 8\sum_{i\neq j}^{nn}\lambda_i\lambda_j. \end{aligned} \tag{B8}$$

Substituting (B7) and (B8) into (B3) one immediately obtains (32).

References

[1] B. Widrow "Adaptive filters," in *Aspects of Network and System Theory*, R. E. Kalman and N. DeClaris, Eds. New York: Holt, Rinehart and Winston, 1970, pp. 563–587.

[2] B. Widrow, P. E. Mantey, L. J. Griffiths, and B. B. Goode, "Adaptive antenna systems," *Proc. IEEE*, pp. 2143–2159, 1967.

[3] L. I. Horowitz and K. D. Senne "Performance advantage of complex LMS for controlling narrow-bank adaptive arrays," *IEEE Trans. Acoustics, Speech, Signal Processing*, vol. ASSP-29, June 1981.

[4] L. J. Griffiths "A simple adaptive algorithm for real-time processing in antenna arrays" *Proc. IEEE*, Oct. 1969.

[5] O. L. Jagerman, "Nonstationary blocking in telephone traffic," *Bell Syst. Tech. J.*, vol. 54, no. 3, Mar. 1975.

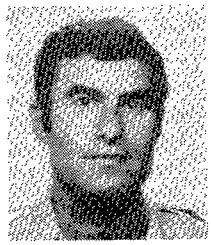

Arie Feuer received the B.Sc. and M.Sc. degrees from the Technion, Haifa, Israel in 1967 and 1973, respectively, and the Ph.D. degree from Yale University, New Haven, CT, in 1978.

From 1967 to 1970, he was employed by Technomatic - Israel, working on factory automation. From 1978 through 1983 with Bell Laboratories, Holmdel, NJ, studying telephone network performance. Since 1983, he has been on the faculty of the Electrical Engineering Department, Technion, Haifa, Israel. His research interests are in adaptive control and adaptive signal processing.

Ehud Weinstein received the B.Sc. degree from the Technion, Haifa, Israel, in 1975 and the M.Sc. and Ph.D. degrees from Yale University, New Haven, CT, in 1976 and 1978, respectively.

In 1978 he joined the Ocean Engineering Department, Woods Hole Oceanographic Institution, where he is currently as Associate Scientist. In 1980 he also joined the Department of Electronic Systems, Faculty of Engineering, Tel-Aviv University, Israel, where he is currently a Senior Lecturer. His research interests are in the area of statistical detection and estimation, and various time-space signal processing problems. He received the IEEE Acoustc Speech and Signal Processing Society 1983 Senior Award.

Root Properties and Convergence Rates of Median Filters

J. PATRICK FITCH, EDWARD J. COYLE, MEMBER, IEEE, AND NEAL C. GALLAGHER, JR., MEMBER, IEEE

Abstract—**Median filters are a special class of ranked order filters used for smoothing signals. Repeated application of the filter on a quantized signal of finite length ultimately results in a sequence, termed a root signal, which is invariant to additional passes of the median filter. In this paper, the theory is developed both for determining the cardinality of the root signal space of arbitrary window width filters applied to signals with any number of quantization levels and for counting or estimating the number of passes required to produce a root for binary signals.**

I. INTRODUCTION

A median filter maps a class of input signals into an associated set of root sequences. Each of these root signals is, by definition, invariant to additional filter passes and is the result of repeated filter passes on one or more of the input signals. One effective use of median filters has been the reduction of high-frequency and impulsive noise in digital images without the extensive blurring and edge destruction associated with linear filters [1]. Other applications include the smoothing of noisy pitch contours in speech signals and data compression using the root signal properties combined with a block truncation coding (BTC) technique [2], [3]. In practice, processing and delay times, possible coding schemes, and output signal space characteristics can all be influenced by both the number of roots and the number of filter passes necessary to reach a root.

The implementation of a median filter requires a simple nonlinear digital operation. To begin, take a sampled signal of length L; across this signal, slide a window that spans $2N+1$ points. The filter output at each window position is given the same position as the sample point at the center of the window and is set equal to the median value of the $2N+1$ signal samples in the window. Start-up and end effects are accounted for by appending N samples to both the beginning and the end of the sequence. The front appended samples are given the value of the first signal sample; similarly, the rear appended samples receive the value of the last sample of the signal. In Fig. 1 we present an example where median filters of window widths three, five, and seven are applied to the same binary sequence. Note that appended bits are denoted by crosses (x) and the window is moved from left to right. The basic idea is to rank the samples in the window and select the median value as the filter output.

Gallagher and Wise [4] obtained some theoretical results relating signal length to the maximum number of filter passes required to reach a root. Because our current work extends these results, several of the definitions and theorems are worth listing here.

1) A *constant neighborhood* is at least $N+1$ consecutive identically valued points.

2) An *edge* is a monotonic region between two constant neighborhoods of different value. The connecting monotonic region cannot contain any constant neighborhood.

3) A *root signal* is a sequence which is invariant to the median filter.

Manuscript received September 12, 1983; revised May 11, 1984. This work was supported by the National Science Foundation under Grants ECS-8306235 and ECS-8203754.

J. P. Fitch was with the School of Electrical Engineering, Purdue University, West Lafayette, IN 47907. He is now with the Engineering Research Division, Lawrence Livermore National Laboratory, Livermore, CA 94550.

E. J. Coyle and N. C. Gallagher, Jr. are with the School of Electrical Engineering, Purdue University, West Lafayette, IN 47907.

0096-3518/85/0200-0230$01.00